ELSEVIER

Colloids and Surfaces
A: Physicochemical and Engineering Aspects 183–185 (2001) 95–111

COLLOIDS AND SURFACES A

www.elsevier.nl/locate/colsurfa

Interaction, critical, percolation and kinetic glass transitions in pluronic L-64 micellar solutions

S.-H. Chen *, C. Liao, E. Fratini [1], P. Baglioni[1], F. Mallamace [2]

Department of Nuclear Engineering, 24-209, Massachusetts Institute of Technology, Cambridge, MA 02139 USA

Abstract

We briefly discuss results of analyses of an extensive set of small angle neutron scattering (SANS) intensity distributions from a class of Pluronic tri-block copolymer micelles in aqueous solutions. This class of Pluronic has a symmetric structure ($PEO_MPPO_NPEO_M$), with PPO/PEO molecular weight ratio of 60/40. It is shown that the micelles are spherical, each consisting of a hydrophobic core and a diffuse hydrophilic corona region having substantial hydration. We use a previously developed 'cap-and-gown' model for the microstructure of the micelle, taking into account the polymer segmental distribution and water penetration profile in the core and corona regions. We treat the inter-micellar correlations using a sticky hard sphere model. With this combination, we are able to fit all SANS intensities satisfactorily for micellar solutions within the range of disordered micellar phase in absolute scale. The structure and interaction of micelle stay is essentially the same as the concentration increases. But the aggregation number and surface stickiness increases, and the micelle becomes less hydrated with increasing temperature. Micellar core is not completely dry but contains up to 20% (volume fraction) of solvent molecules at lower temperatures. We then discuss, in some details, Pluronic L64 ($PEO_{13}PPO_{30}PEO_{13}$) micellar system. This system shows an inverted bi-nodal line with a lower critical consolute point and a percolation line. We investigated the structure and interaction between these micelles as temperature approaches the bi-nodal line along iso-concentration lines. The model developed above is able to describe SANS data in critical region also satisfactorily. As one approaches the bi-nodal line at constant weight fraction of the copolymer, the aggregation number and the stickiness parameter increase. In particular, at weight fraction of 5%, the stickiness parameter approaches the critical value 10.2 at $T = 330.9$ K. We investigated the effect of hydrophobic impurities in the commercial polymer on the critical phenomenon. We conclude that in both the pure and impure systems, the micellar solution shows a critical demixing point where micelles stay spherical but interact strongly with each other by a short range temperature dependent attraction. Furthermore, from this fitting procedure we find relationships between the stickiness parameter and temperature, the volume fraction of micelles and the polymer concentration. Using these two relations, we are able to map the phase diagram of the sticky sphere model onto that of the micellar solution. The agreement between the

* Corresponding author: Tel.: +1-617-2533810; fax: +1-617-2588863.
E-mail address: sowhsin@mit.edu (S.-H. Chen).
[1] Permanent address: Department of Chemistry and C.S.G.I., Universita' di Firenze, Via G.Capponi 9, 50121 Firenze, Italy.
[2] Permanent address: Department of Physics and Istituto Nazionale Fisica della Materia, Universita' di Messina, Vill. S. Agata C.P. 55, 98166 Messina, Italy.

PII: S0927-7757(01)00542-8

theory and experimental phase behavior is satisfactory. Finally, we briefly describe the recently found kinetic glass transition line in this system using a scaling plot of SANS data below and above the transition.

Keywords: Interaction; percolation; kinetic glass transitions

1. Introduction

Polyethylene oxide and polypropylene oxide containing block copolymers belong to a class of polymers that associate spontaneously in aqueous solution. The self-association is characterized by sensitivity to temperature [1]. In particular, many tri-block copolymers composed of two symmetric end-block polyethylene oxides and a middle-block polypropylene oxide have been synthesized and used as polymeric surfactants. These tri-block copolymers we studied are commercially available under a trade name Pluronic from BASF [2]. Pluronic polymer surfactants find widespread industrial applications as detergents, wetting, foaming/defoaming, emulsification, lubrication and solublization agents [2–4].

The most interesting feature of the Pluronic polymer is its ability to self-associate in aqueous solutions and the resultant rich phase behavior of the solutions [3,5–12]. At low polymer concentrations and low temperatures, the tri-block copolymers in water exist as single-coils, called unimers. At moderately high concentrations or temperatures, the copolymer molecules self-associate to form thermodynamically stable aggregates-micelles. The micelles exist in a disordered phase within substantial temperature and concentration ranges. At even higher concentrations and temperatures, the copolymer chain and micelles can form ordered phases, such as cubic, hexagonal and lamellar phases [5,11,12]. The self-assembly and phase behavior of the copolymer solution depends on the total molecular weight and the relative PPO/PEO composition of the copolymer.

Micellization occurs above a critical micellization temperature which is a function of concentration (called cmt and cmc, respectively). Dynamic light scattering shows that Pluronic micellar solutions exhibit significant polydispersity at low temperatures, near cmt, but become monodisperse at high temperatures [6]. Batch-to-batch of the surfactant supplied contains variable composition heterogeneities, such as di-block copolymer impurities. These impurities may considerably affect the initial micelle formation and surface tension, but have less effect on the micellar structure and inter-micellar interaction for concentrations beyond the cmt/cmc line. We, therefore, confine our study of the microstructure and interaction of micelles far beyond micellization boundary where we may ignore such impurities and heterogeneities.

In this paper, we focus our attention on a particular class of Pluronic surfactant family, i.e. copolymers containing 40–60 molecular weight ratio of polyethylene oxides and polypropylene oxide. This class of Pluronic has several members, namely, P104, P94, P84, L64 and L44, with decreasing molecular weight. Out of these five, we selected P104, P84 and L64 in particular for a more detailed study. Molecular weights and molecular volumes of P104, P84 and L64 are given in Table 1.

In order to determine the range of the disordered micelle phase, it is important to measure its two boundaries, i.e. the micellization at low concentration and gelation at high concentration. The experimental cmt–cmc boundaries of the Pluronic P104, P84 and L64 in aqueous solutions are determined using light scattering method [13]. Micelles are formed as temperature or concentration increases beyond the cmt–cmc line. This causes an abrupt increase of light scattering signal.

For surfactants with the same PEO–PPO composition, higher molecular weight polymers tend to form micelles at lower concentration and/or temperature. Gelation of Pluronic solutions occurs at high polymer concentrations. For the 40% PEO Pluronic family, concentration of the sol–gel transition is only slightly dependent on tempera-

ture. The micellization and sol–gel transition are correlated, higher cmc tends to correspond to higher gelation concentration. However, the sol–gel boundary is nearly vertical on the phase diagram. For stable micellar solutions at temperatures higher than 30°C, the variation of gelation concentration is normally at most 1 or 2 wt.% within a large temperature range. The gelation concentrations for Pluronic P104 and P84 are 20 and 22 wt.%, respectively. These gelation concentrations set the upper limit for the concentration ranges of the disordered micellar phases. The disordered micellar phase has an upper temperature boundary called cloud points. The cloud points of micellar solutions of P84 and P104 are 75 and 85°C showing little concentration dependence.

2. The model for the micellar structure factor

We assume that the micelle has a compact spherical hydrophobic core of radius a, consisting entirely of PPO segments with the polymer volume fraction ϕ_p (and water volume fraction $1-\phi_p$), and a diffuse corona region, consisting of all PEO segments and water of hydration. Since hydrophilicity of the PPO segments becomes significantly less than that of the PEO only at elevated temperatures, this assumption of purely PPO segregated core may not be valid near cmc–cmt line. The radial profile of PEO segmental distribution in corona region is assumed to be Gaussian with a width σ. The overall polymer segmental distribution in the micelle is thus expressed as [14] (note the slight difference in the definition of $\phi_p(r)$ from [14]):

$$\phi_p(r) = \begin{cases} \phi_p & \text{for } 0 < r < a \\ \phi_p \exp\left(-\dfrac{r^2}{\sigma^2}\right) & \text{for } a < r < \infty \end{cases} \quad (1)$$

The neutron scattering length density profile can then be calculated in terms of the known scattering length densities of polymer ρ_p, and water, ρ_w, as

$$\rho(r) = (1-\phi_p(r))\rho_w + \phi_p(r)\rho_p \quad (2)$$

The difference, $\Delta\rho(r) = \rho(r) - \rho_w$, between the scattering length density of polymers and that of the solvent (the contrast) determines the particle structure factor.

$$F(k) = \int d^3r \Delta\rho(r) \exp(i\vec{k}\bullet\vec{r}) = \frac{4\pi a^2}{k}(\rho_p - \rho_w) \times \phi_p\left[j_1(ka) + \int_1^\infty dX X \sin(kaX)\exp(-t^2X^2) \right] \quad (3)$$

The core radius a, the Gaussian width σ and the polymer volume fraction in the core ϕ_P are related by two geometrical constraints. The total volume of polymer segments in the core is given by the product of the aggregation number N and PPO segmental volume $v_{PPO} = 95.4 \times 30$ Å^3. Similarly, the total volume of polymer segments out-

Table 1
Molecular volumes, scattering lengths and scattering length densities of polymers and solvent

	Chemical formula	Molecular weight	Molecular volume (Å^3)	Scatt. lengths Σb_i (fm)	Scatt. Length density (10^{-6} Å^2)
EO	$-(CH_2)_2O-$	44	72.4	4.14	0.572
PO	$-(CH_2)_3O-$	58	95.4	3.31	0.347
Solvent	D_2O	20	30.3	19.153	6.321
P104	$PEO_{27}PPO_{61}PEO_{27}$	5900	9706	424.1	0.437
P84	$PEO_{19}PPO_{43}PEO_{19}$	4200	6920	302.1	0.437
L64	$PEO_{13}PPO_{30}PEO_{13}$	2900	4744	206.9	0.437

side the core is given by the product of aggregation number N and PEO segmental volume $v_{PEO} = 72.4 \times 26$ Å^3. Combining these two constraints, we can write

$$\frac{v_{PEO}}{v_{PPO}} = \frac{3\int_t^\infty X^2 dX \exp(-X^2)}{t^3} = 0.685 \quad (4)$$

where, we define the ratio of the core radius a to the Gaussian width as $t = a/\sigma$. This constraint results in the value of $t = 1.03$. It is more convenient to define a normalized form factor by dividing $F(k)$ by its $k = 0$ value

$$F(0) = (\rho_p - \rho_w)(V_p^{core} + V_p^{corona})$$
$$= (\rho_p - \rho_w)\frac{4\pi a^3}{3}\phi_p\left(1 + \frac{v_{PEO}}{v_{PPO}}\right) \quad (5)$$

The normalized form factor is

$$\tilde{F}(k) = \frac{F(k)}{F(0)}$$
$$= \frac{v_{PPO}}{v_{PPO} + v_{PEO}}\left[\frac{3j_1(ka)}{ka} + 3\int_1^\infty dX X \frac{\sin(kaX)}{ka}\exp(-t^2X^2)\right] \quad (6)$$

which depends only on one parameter a. The normalized particle structure factor is $\tilde{P}(k) = |\tilde{F}(k)|^2$.

3. The model for the inter-micellar structure factor

The intermicellar interaction is taken to be consisting of a hard core of diameter R and a short range attraction of a depth $-\varepsilon$ and a range of Δ Baxter [15] showed that the Ornstein–Zernike equation for this square well potential can be solved analytically in Percus–Yevick approximation [16] by taking a limit $\Delta \to 0$, $\varepsilon \to \infty$, in such a way that the stickiness parameter $1/\tau = (12\Delta/R)\exp(\beta\varepsilon)$ is finite. The analytic solution of the inter-particle structure factor $S(k)$ is expressed as a function of the hard sphere volume fraction ϕ, the hard sphere diameter R and the stickiness parameter $1/\tau$ as [14]:

$$\frac{1}{S(X)} - 1 = 24\phi\left[\alpha f_2 + \beta f_3(X) + \frac{1}{2}\alpha\phi f_5(X)\right] + 2\phi^2\lambda^2 f_1(X) - 2\phi\lambda f_0(X) \quad (7)$$

where $x = kR$ and various functions are defined as $f_0(x) = \sin(x)/x$; $f_1(x) = (1 - \cos(x))/x^2$; $f_2(x) = (\sin(x) - x\cos(x))/x^3$; $f_3(x) = (2x\sin(x) - (x^2 - 2)\cos(x) - 2)/x^4$; $f_5(x) = ((4x^3 - 24x)\sin(x) - (x^4 - 12x^2 + 24)\cos(x) + 24/x^6$. The parameters in Eq. (7) are defined as

$$\lambda = \frac{6}{\phi}\left[\tau + \frac{\phi}{1-\phi} - \sqrt{\left(\tau + \frac{\phi}{1-\phi}\right)^2 - \frac{\phi(1+\phi/2)}{3(1-\phi)^2}}\right]$$
$$\mu = \lambda\phi(1-\phi)$$
$$\alpha = \frac{(1+2\phi-\mu)^2}{(1-\phi)^4}$$
$$\beta = -\frac{3\phi(2+\phi)^2 - 2\mu(1+7\phi+\phi^2) + \mu^2(2+\phi)}{2(1-\phi^4)} \quad (8)$$

From the limiting value of the structure factor $S(k->0) = \rho k_B T \chi_{T,}$ one can get the isothermal compressibility χ_T .By integrating $\chi_{T,}$ one can obtain the compressibility equation of state. From the equation of state, and a known analytical expression for the chemical potential [17] one can determine the coexistence curve between the liquid and gas. The liquid–gas critical point occurs at, $1/\tau_c = 6/(2 - \sqrt{2}) = 10.25$, $\phi_c = (3\sqrt{2} - 4)/2 = 0.1213$.

When approaching the critical point along the critical isochore, the Eq. (7) can be simplified in the low k limit by expanding the parameters λ, μ, α, and β in terms of the reduced parameter $t = (1 - \tau_c/\tau)^{1/2}$ around the critical point, and maintaining the terms up to the second order in t and k. The resultant form is the well known Lorentzian function in k,

$$S(k) = \frac{\rho k_B T \chi_T}{1 + k^2\xi^2}, \quad (9)$$

where the long range correlation length ξ, and the isothermal compressibility χ_T are given by,

$$\xi = \sqrt{\frac{3}{40 - 28\sqrt{2}}}R\left(1 - \frac{\tau_c}{\tau}\right)^{-1/2},$$
$$\rho k_B T \chi_T = \frac{27}{4 - 2\sqrt{2}}\left(1 - \frac{\tau_c}{\tau}\right)^{-1}. \quad (10)$$

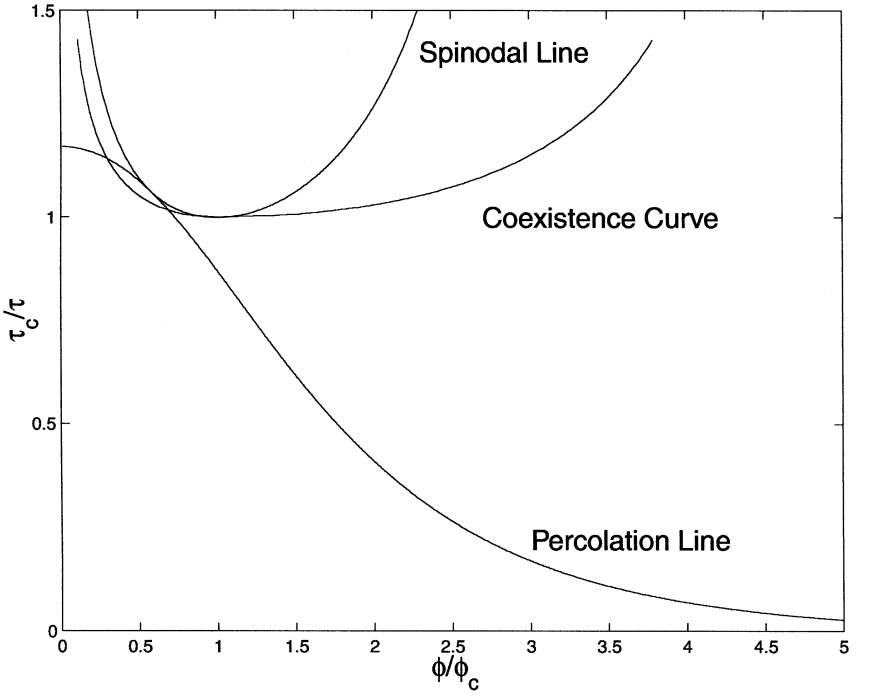

Fig. 1. The phase diagram of Sticky Hard Sphere model. The critical stickiness is, $1/\tau_c = 10.25$, and the critical volume fraction, $\phi_c = 0.1213$. Percolation line is defined by Eq. (11).

The correlation length ξ is proportional to the hard sphere diameter R and diverges with a power-law exponent v, while the isothermal compressibility with an exponent γ when the stickiness approaches the critical value. The exponents $v = 1/2$, and $\gamma = 1$ agree with prediction of the mean field theory if we assume the reduced stickiness $1 - \tau_c/\tau$ is proportional to the reduced temperature$1 - T/T_c$.

One of the novelties of Baxter model is that one can introduce in a natural way the concept of connectedness of two spheres and thus a cluster. It has then a well defined percolation threshold. Chiew and Glandt [18] defined the percolation threshold as the points on the phase diagram ($1/\tau$, ϕ space) where the average cluster size of the system diverges. The loci of the percolation are given by an analytical expression:

$$\frac{1}{\tau} = \frac{12(1-\phi)^2}{19\phi^2 - 2\phi + 1} \tag{11}$$

Fig. 1 gives the theoretical phase diagram of the Baxter model [19]. One sees a rather flat inverted coexistence line lying in the upper left hand corner and a percolation line, starting from the vicinity of the critical point, where the stickiness is the maximum, cutting across the phase plane from left to right, progressively in the direction of decreasing stickiness.

4. Summary of the results

SANS scattering intensity $I(k)$ (in unit of cm^{-1}), where k is the magnitude of the scattering vector, is proportional to a product of the normalized particle structure factor $\bar{P}(k)$ and the inter-particle structure factor $S(k)$, both dimensionless. The constant factor in front of it is a product of the polymer concentration $C = c - \text{cmc}$ (c, grams of polymer molecules per ml), the contrast factor square, and the aggregation number of a micelle N [20]. In the contrast factor within the square bracket, the first term is the sum of coherent scattering lengths of atoms comprised of a polymer

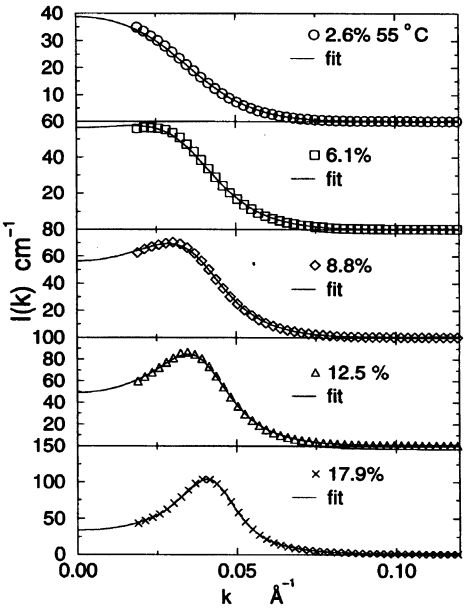

Fig. 2. SANS data from Pluronic P 84 micellar solutions in D_2O at 55°C, at various concentrations and their model fits.

molecule, ρ_w the scattering length density of the solvent and v_m the polymer molecular volume. The complete formula for scattering intensity from a system of monodisperse micelles is

$$I(k) = \frac{CN_A}{M_P}\left[\sum_i b_i - \rho_w v_m\right]^2 N\bar{P}(k)S(k) \qquad (12)$$

where N_A is the Avogadro number and M_p the molecular weight of the polymer. It is important to note that the absolute intensity is directly proportional to the aggregation number N. The polymer concentration and the contrast factor are known quantities.

In our model, the four primary fitting parameters are: the aggregation number of a micelle N, the outer micellar diameter R (or alternatively, the volume fraction of micelles ϕ), the stickiness parameter $1/\tau$, and the polymer volume fraction in the micellar core ϕ_p. Other parameters, such as the total hydration number H (number of water molecules attached to a polymer in a micelle), the volume fraction of micelles ϕ or alternatively, the outer diameter of the micelle R, core radius a, Gaussian tail width σ, and the hydration numbers in the core H_c, are uniquely related to the four primary parameters. The more sensitive parameters of the fit are the aggregation number N, the volume fraction ϕ, and the micellar diameter R. The aggregation number determines the overall amplitude of the scattering intensity and can be obtained by fitting SANS data in an absolute intensity scale. The volume fraction of micelles controls the peak height of the structure factor $S(k)$. The micellar diameter determines the peak position of $S(k)$. These three parameters basically decide the general shape and amplitude of $I(k)$. Two less sensitive parameters determine the detailed rise and fall of the scattering peak and small and large k behaviors of the scattering intensity. These parameters are the stickiness and the polymer volume fraction in the core. A Fortran code based on a gradient searching non-linear least square fitting method [21] was developed and used to fit SANS intensities in an absolute scale. Quality of the fits is uniformly excellent for Pluronic micellar systems within the range of disordered micellar phases. To show the goodness of the fits, a set of concentration series taken for P84 at a temperature 55°C and their fits are shown in Fig. 2. The parameters extracted from the fittings are shown in Table 2.

Table 2
Parameters for the microstructure and interaction of P84 polymeric micelles at 55°C extracted from SANS intensities

Concentration (wt.%)	Aggregation number N	Hydration N H	$1/\tau$	Diameter R (Å)	ϕ_p	Core radius a (Å)	Micelle VF ϕ
2.6	81	142	0.48	145	0.93	44	0.05
6.1	80	126	0.47	145	0.95	44	0.10
8.8	80	134	0.45	146	0.94	43	0.15
12.5	79	130	0.43	146	0.96	43	0.21
17.9	78	129	0.47	142	0.95	43	0.29

Table 3
Parameters of the microstructure and interaction of P84 polymeric micelles extracted from SANS intensities

Temperature (°C)	Aggregation N	Hydration H	Core radius a (Å)	Micellar diameter R (Å)	$1/\tau$
35	44	240	37	105	0.10
40	54	210	38	108	0.25
45	66	190	40	115	0.35
55	80	130	43	118	0.45

Table 4
Parameters of the microstructure and interaction of P104 polymeric micelles extracted from SANS intensities

Temperature (°C)	Aggregation N	Micellar hydration H	Diameter Core radius		Core hydration H_c	$1/\tau$
			R (Å)	a (Å)		
45	84	627	166	49.7	10.2	0.10
50	106	500	171	3.7	10.4	0.29
55	120	597	185	56.0	10.2	0.50

Listings on the above table show that at a given temperature, ratio between the volume fraction of micelles to the volume fraction of dry surfactant molecules at different concentrations is a constant. The stickiness parameter characterizing the interaction is also a constant. Furthermore, the aggregation number and the structural parameters of the micelle are independent of concentration. This leads us to conclude that, in contrast to typical ionic micellar systems, the microstructure and interaction of non-ionic micelles formed by tri-block copolymers of PEO and PPO are determined only by temperature, independent of the polymer concentration. We can thus summarize the temperature dependence of a number of the more interesting parameters, averaged over a range of concentrations, for P84 and P104 micellar systems in Tables 3 and 4.

The hydration number decreases with temperature as the micelles become more compact at high temperatures. The hydrated water molecules take up a large fraction of volume in a micelle. For example, for Pluronic P84 micelle at an intermediate temperature, the hydration number for each polymer chain is 240. Knowing the specific volume of a water molecule (30 $Å^3$) and the molecular volume of P84 (6920 $Å^3$), we obtain the volume ratio of hydrated water to polymer in a P84 micelle to be about 1.05. This means that more than 50% of the micellar volume is occupied by solvent molecules. The effect of hydration thus contributes significantly to the properties of the micellar solution. SANS analysis also gives the stickiness parameter. The trend of the stickiness parameter indicates that at low temperatures, the micelles are close to hard spheres. The surface of the micelles become stickier as micelles grow at elevated temperatures. This effect is consistent with increased hydrophobicity of the polymers at elevated temperatures. Water penetration profile is an interesting result. The micelle has regions of core and shell with distinctly different polymer and solvent volume fractions. The core of a Pluronic micelle is not completely dry, in agreement with theoretical predictions [22]. The polymer volume fraction in the core is about 92–97% at higher temperatures, independent of temperature and concentration. This suggests that only at most 8% of volume inside the core is occupied by the solvent. However, at low temperatures the water penetration seems to depend on the concentration. For P84 at 35°C, polymer volume fraction in the core goes from 80% at concentration of 2.6 wt.%, up to 96% at concentration of 18 wt.%. It can be concluded that at high temperatures, the polymeric micelle becomes more com-

pact. It has a larger association number but smaller hydration number.

5. Critical and percolation transitions in L64/water system

We shall discuss in this section Pluronic L64 (PEO_{13} PPO_{30} PEO_{13}) micellar system since it has a phase diagram which can be mapped into that of the sticky sphere model system. Al-Saden and co-workers investigated the aggregation behavior of L64 in water by photon correlation spectroscopy [23]. They detected micellar aggregates at 25°C only at concentrations above approx. 6%. The aggregation number exhibited a significant polydispersity at this temperature. But at 35°C, the micelles become monodisperse. Zhou and Chu found [24] that the micelle formation shifted markedly to lower concentrations and micelles grow larger as a function of temperature. Pandya et al.[25] further claimed that micelles grow significantly larger near the cloud points. We shall show below that the scattering intensity in small k region increases markedly near the cloud points because of critical fluctuations.

Fig. 3 is the phase diagram of Pluronic L64/D_2O micellar solution determined by combination of several methods: direct observation of the phase behavior; static and dynamic light scattering experiments; SANS experiments; and viscosity measurements [26]. The temperature and concentration dependent percolation threshold can be detected by a jump (about two orders of magnitude) in shear viscosity. Using the SANS technique, we investigated temperature dependence of the microstructure of the copolymer micelles and the interaction among these micelles at a wide

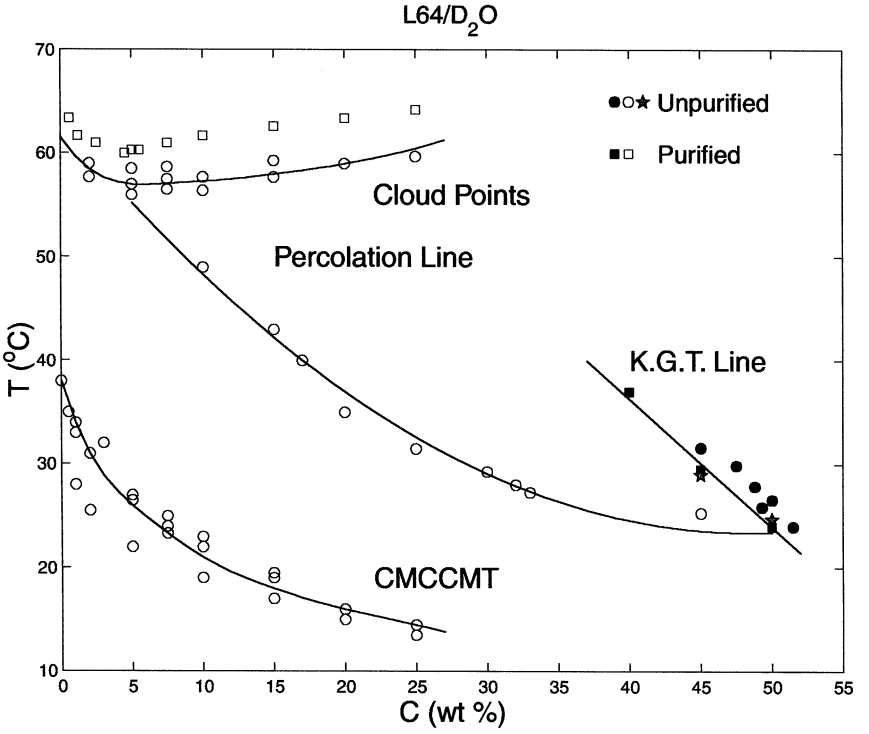

Fig. 3. The phase diagram of Pluronic L64 in D_2O solution. The phase diagram contains: the cmc–cmt line, the bi-nodal lines or cloud point curves (both for commercial and purified samples), the percolation line (for commercial sample) and locus of kinetic glass transition lines (for both commercial and purified samples). Symbols are values determined by a direct observation of phase separation behavior, light and neutron scattering and viscosity measurements. Solid lines are drawn to guide the eyes.

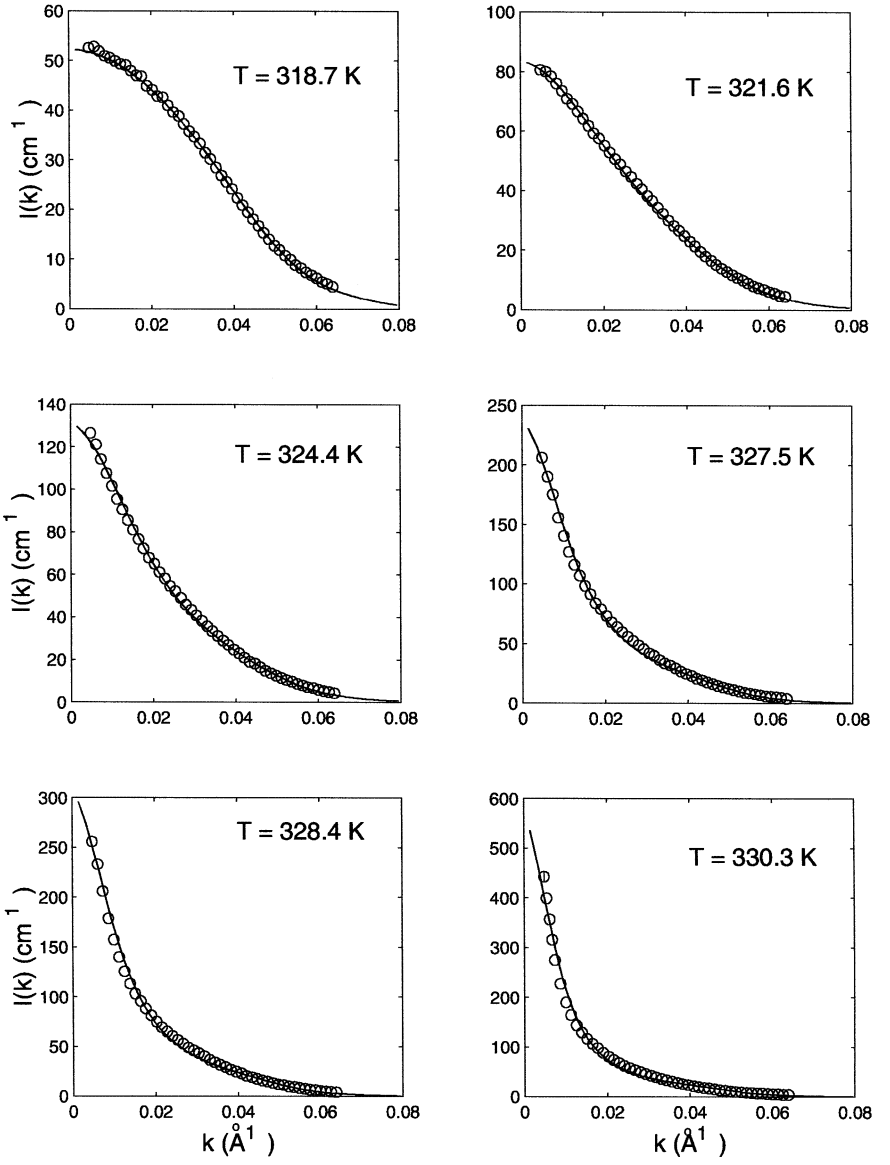

Fig. 4. SANS data (symbols) and their model fits (solid lines) for Pluronic L64 (commercial grade) micellar solutions in D_2O at 5.0 wt.% and different temperatures. $T_c = 330.3 \pm 0.5$ K.

range of concentrations (2.5–50 wt.%) and at temperatures much higher than the critical micellization temperature but lower than the cloud points. Based on combination of Cap-and Gown and sticky hard sphere model and its analysis of SANS data, at temperature–concentration range much above the cmc–cmt line, we verified that the copolymer aggregates exist as spherical micelles with a high degree of monodispersity. Fig. 4 shows SANS scattering intensity distributions and their model fits at copolymer concentrations of 5.0 wt.%. We are aware that some earlier literatures [27,28] showed the presence of a systematic deviation from sphere-shape micelles, in Pluronic

P85/water system at elevated temperatures, by calculating the pair-correlation function from Fourier transform of the scattering intensity distribution. However, we comment here that for L64, even at low polymer concentration (such as 5 wt.%), the intermicellar attractive interaction can not be ignored and its influence on the scattering distribution becomes more significant at elevated temperatures. The increase of the stickiness as temperature, which can be seen from Fig. 5,

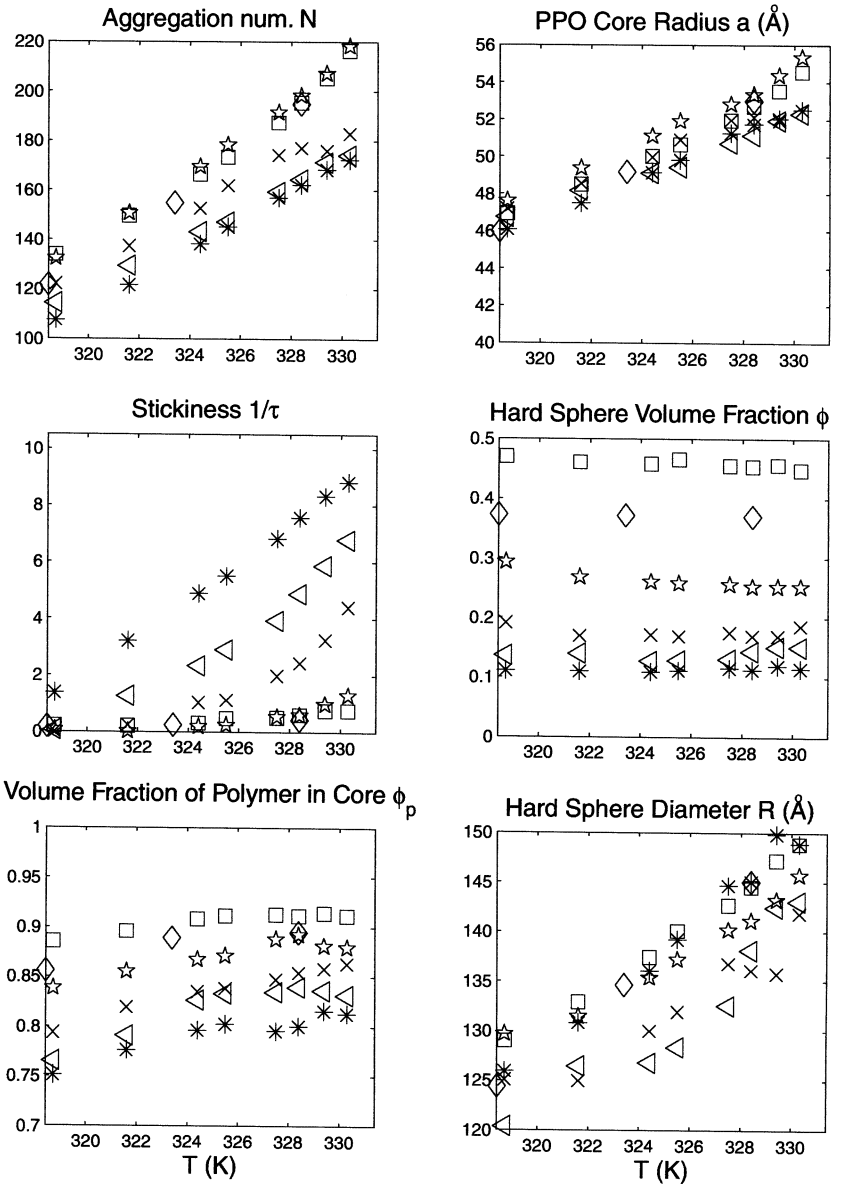

Fig. 5. Summary of the physical parameters extracted from SANS data of Pluronic L64 (commercial grade) micellar solutions in D_2O. The top four boxes are the four primary fitting parameters. The volume fraction of polymer in the core ϕ_p and the hard sphere diameter R are calculated from these four primary fitting parameters. Different symbols in each box denote different concentrations: squares represent 25.0 wt.%, diamonds 20.0 wt.%, stars 15 wt.%, crosses 10.0 wt.%, triangles 7.5 wt.%, and asterisks 5.0 wt.%.

causes the low angle scattering intensity to increase. In particular, along the critical concentration (around 5.0 wt.%), the $k=0$ intensity becomes divergent as temperature approaches the critical consolute point at $T=330.3$ K, where the stickiness parameter approaches the critical value 10.23. Away from the critical concentration, the low angle intensities only increase moderately as temperature approaches the cloud point line.

Fig. 5 summarizes the parameters extracted from the model fits of all SANS data for Pluronic L64/D_2O solutions. The plots give the variations of the parameters as a function of temperature for different copolymer concentrations. As temperature increases, the aggregation number and core radius increase linearly. The stickiness parameter increases to the critical value according to a power law for samples having concentrations in the range of 2.5–10 wt.%. For a sample at 15 and 25 wt.%, the stickiness increases slowly always below the value of 1.0. Temperature dependence of the volume fraction is weak, and the relation between hard sphere volume fraction ϕ and the copolymer concentration c follows a simple relation, $\phi=1.8\ c$. We shall call it the first scaling law. The volume fraction of polymer in the core is derived from the geometrical constraints and increases slowly with temperature indicating that the micellar core becomes drier. This result is consistent with the fact that PPO becomes less hydrophilic when heated. At this point, it would be relevant to investigate the effects of hydrophobic impurities known to be present in commercial L64 samples available from BASF on the critical phenomenon. We, therefore, purify the commercial grade sample according to a procedure described in [29]. Pluronic L64 was received as a gift from BASF. The copolymer was purified by extraction with hexane fractions [29] according to the following procedure. About 10 g of copolymers was dispersed in 25 ml of hexane by stirring at room temperature (20°C) for 2 h. The phases were allowed to separate, and the upper hexane phase was discarded. This procedure was repeated four times. The liquid copolymer was then submitted to rotational evaporation under moderate vacuum (10 mmHg) for 3 h at 5°C, to remove most of the hexane. The resulting liquid was then dried overnight on a vacuum pump to remove any trace of residual solvent. The purity of Pluronic was checked by chromatography and by atomic adsorption to detect the possible presence of hydrophobic compounds (mostly di-block copolymers, P84 and P104) and salts. In the purified L64 we detected the following cations: $Na^+=3$ ppm, $K^+=3$ ppm, and $Ca^{2+}=1$ ppm. Due to the very low amount of these cations no further purification from ionic impurities has been performed. The presence of hydrophobic impurities was also checked by measuring the absorbance at 360 nm of a 2.5% (w/v) solution of L64 in H_2O (Milli-Q water Organex system), and in the temperature range 20–60°C, by using a Perkin–Elmer 900 Vis-UV spectrometer. The temperature has been increased at a rate of 0.2°C/min. After the purification procedure, L64 does not show peaks below the cmt [30], that are present in the unpurified samples, indicating that the hydrophobic impurities were no longer present in the block-copolymer.

SANS measurements were repeated for the purified sample at concentrations 4.5, 5.0 and 5.5 wt.%. Results of the same analyses were shown in Fig. 6. It is seen that $1/\tau$ versus T curves are still linear and ϕ versus c curves flat in temperature. Thus characteristics of the critical scattering for the purified sample remains qualitatively similar to that of the commercial grade sample, provided one allows for slight shifts in the critical concentration and critical temperature. Judging from the parameters listed in Fig. 6, the critical concentration for the purified sample is closer to 4.5 wt.% and the critical temperature is 333.4 K (Fig. 3).

The long-range correlation length ξ along the critical isochore in the sticky hard sphere system can be calculated from Eq. (10). It is given in Fig. 7 for the commercial grade sample where we use the stickiness and hard sphere diameter obtained by fitting of SANS data at the critical concentration of 5.0 wt.%. The experimental values for the correlation length given in Fig. 7 are then compared with the general expression along the critical isochore:

$$\xi=\xi_0\left(1-\frac{T}{T_c}\right)^{-\upsilon}. \tag{13}$$

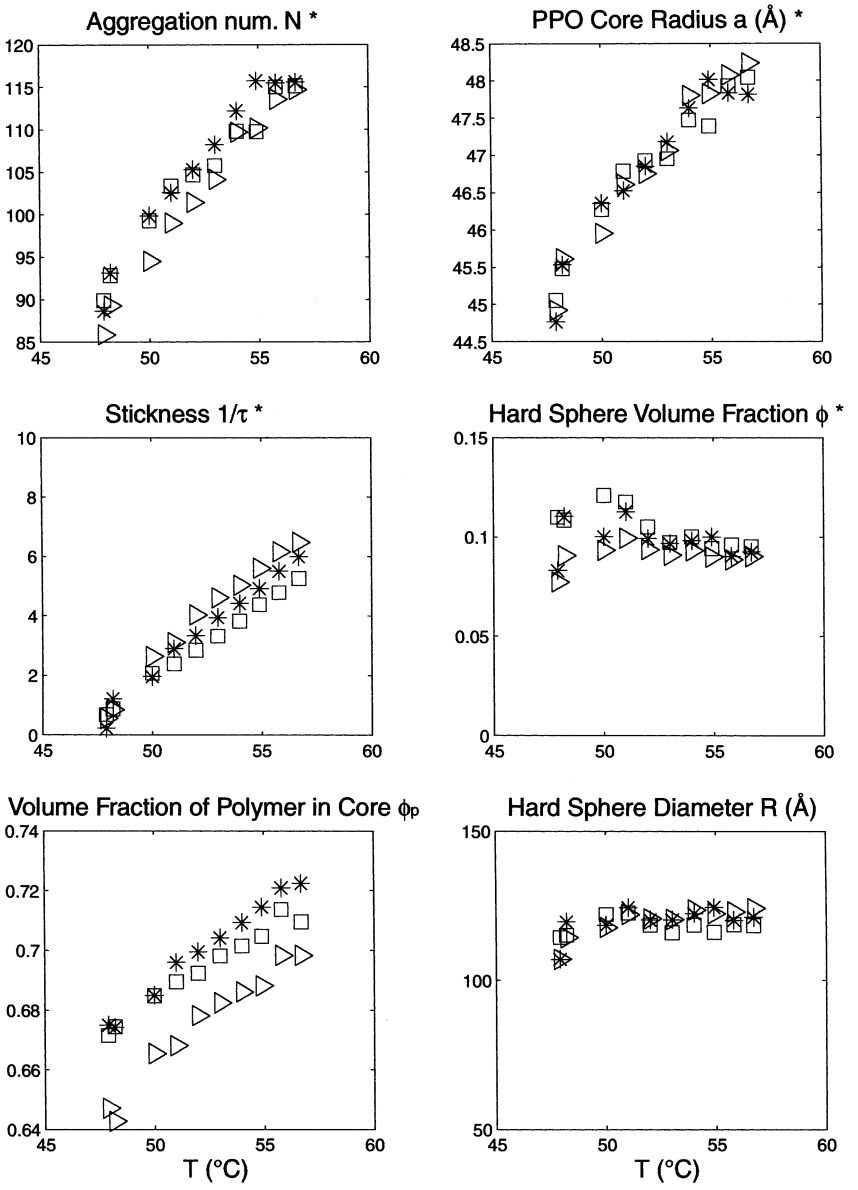

Fig. 6. Summary of the physical parameters extracted from SANS data of Pluronic L64 (purified) micellar solutions in D_2O. The top four boxes indicated with an asterisk are the four primary fitting parameters. The volume fraction of polymer in the core ϕ_p and the hard sphere diameter R are calculated from these four primary fitting parameters. Different symbols in each box denote different concentrations: triangles represent 4.5 wt.%, asterisks 5.0 wt.% and squares 5.5 wt.%.

From which we obtain the short-range correlation length $\xi_0 = 61$ Å, and the critical exponent $v = 0.56 \pm 0.08$. These values agree with that obtained from light scattering experiments [26], where these values are calculated from variations of compressibility with temperatures. By comparing Eq. (13) with the correlation length expression of Eq. (10) obtained from the sticky hard sphere model, we get an empirical relation [31]:

$$\left(1-\frac{\tau_c}{\tau}\right)=\alpha\left(1-\frac{T}{T_c}\right)^{\gamma} \quad (14)$$

with $\gamma = 2v$ If we ignore the weak temperature and concentration dependence of the multiplicative constant α, and the exponent γ, we could call this the second scaling law. One can then use the two scaling laws derived above to map the phase diagram of the sticky hard sphere system (Fig. 1) from the $(1/\tau, \phi)$ plane to the (T, c) plane. The resultant phase diagram can then be compared with the experimental phase diagram of L64/D_2O solution shown previously in Fig. 3. The mapping is represented as the solid line in Fig. 8. The value of γ satisfies the known scaling relation $\gamma = 2v$. The agreement between theory and experimental phase diagrams is fair.

Recently, we found an interesting dynamic, ergodic to non-ergodic transition in intermediate scattering functions as measured by photon correlation spectroscopy [32]. The loci in the phase diagram where this dynamic transition occurs are indicated by solid circles in Fig. 3. The photon correlation measurements were made on the commercial grade sample. We then examined a series of SANS intensities taken from the commercial grade and purified samples in this area of the phase diagram. It turns out that both the commercial grade and purified samples show similar behavior. Fig. 9 shows a scaling plot of a micellar solution made with $c = 50$ wt.% at a series of temperatures ranging from 17.0 to 46.8°C. The scaling plot has an advantage that transition in line width can be easily visualized. It is clear from this plot that a sudden narrowing of the line width occurs at about 22.5°C. From 2-D patterns of the SANS intensity distributions, we know this is an amorphous-to-amorphous structural transition (absence of spots in the 2-D intensity pattern). Solid line in Fig. 9 represents k-resolution of the SANS spectrometer used. The line shape is

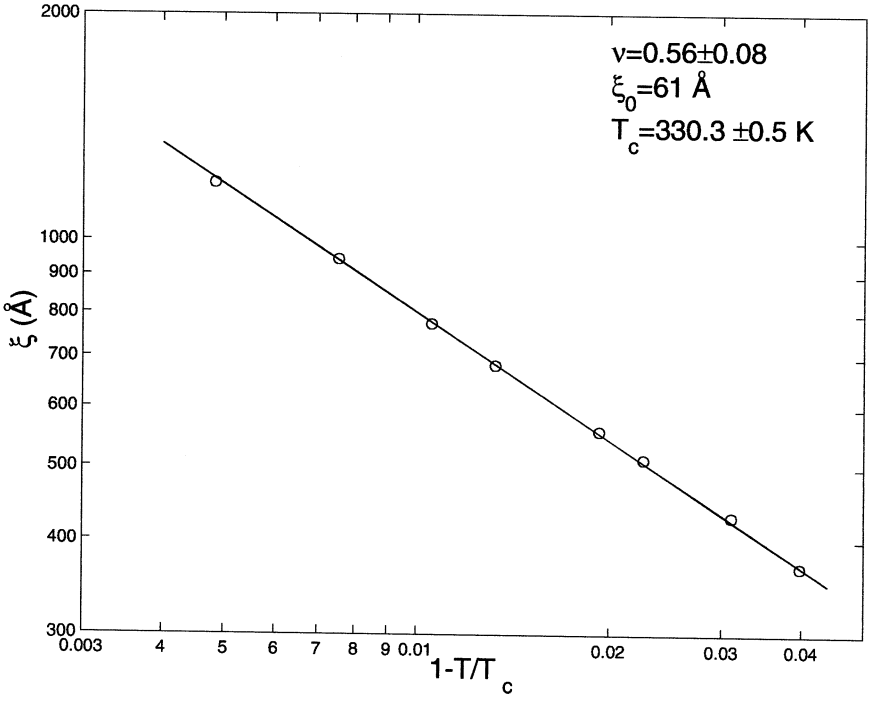

Fig. 7. Temperature dependence of the long-range correlation length (symbols) along the critical concentration (commercial grade, 5.0 wt.%) calculated by Eq. (10) using values of the hard sphere diameter R and stickiness parameter $1/\tau$ taken from fitting of the corresponding scattering intensity distributions (Fig. 5). The solid line is the curve $\xi = \xi_0(1 - T/T_c)^{-v}$ with $\xi_0 = 61$ Å, $v = 0.56 \pm 0.08$, and $T_c = 330.3 \pm 0.5$ K. Note the exceptionally large value of ξ_0.

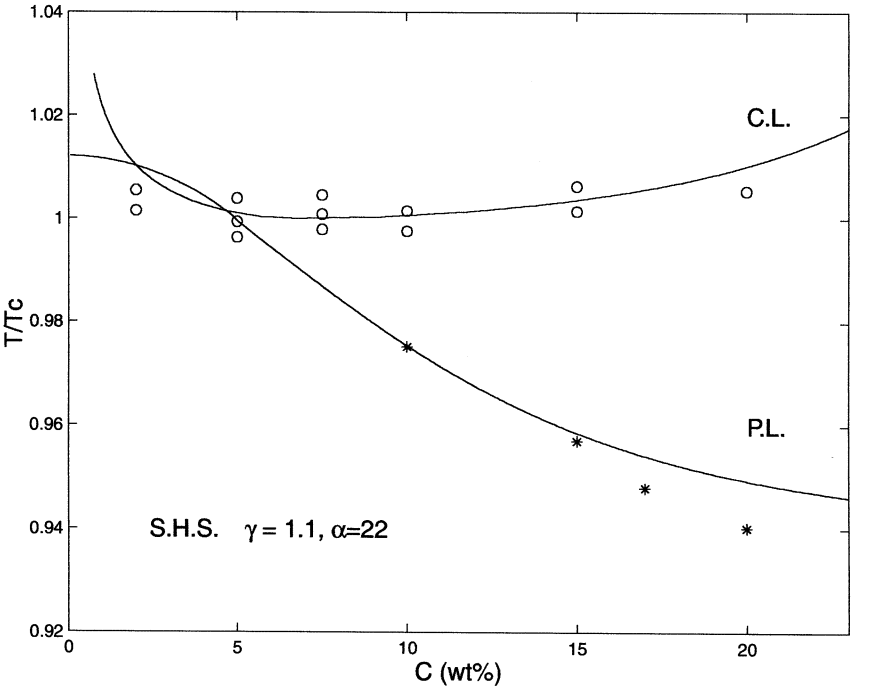

Fig. 8. Comparison of the theoretical phase diagram for Sticky Hard Sphere model (solid line) with that of the experimental one for Pluronic L64/D_2O micellar solutions (symbols, commercial grade). In order to transform the coordinates (ϕ, $1/\tau$) in the sticky hard sphere model to the corresponding experimental coordinates (c, T), we used two scaling relations: $\phi = 1.8 \times c$ and $|1 - \tau_c/\tau| = \alpha|1 - T/T_c|^{\gamma}$, with $\alpha = 22$ and $\gamma = 1.1$.

very well approximated by a Lorentzian. Fig. 10 depicts the half width of the Lorentzian line versus temperature for three L64 concentrations. Sharp breaks in line widths occur at a characteristic temperature for a given concentration. Dotted line represents width of the resolution. It shows that above the transition, the line width is nearly resolution-limited. In this scaling plot, the position of the peak (originates from the first diffraction peak in the liquid structure factor) reflects the mean particle separation in the liquid-like ordering of the system. The peak sharpens when the near neighbor distances becomes more uniform. The loci of this transition are represented by squares in the phase diagram shown in Fig. 3. Thus, the previously discovered ergodic-to-nonergodic dynamic transition seems to be accompanied by a structural ordering as well.

6. Conclusion

We have shown from analyses of an extensive set of SANS data taken along iso-concentration lines in the disordered micellar phase that there is a critical demixing point existing within the cloud point curve of L64/D_2O system. The critical concentration is in the vicinity of 4.5–5 wt.%, depending on purity of the copolymer. The critical temperature in the purified sample is higher by about 2.5 K. For the concentration range we studied, the structure of micelles stays spherical as one approaches the cloud points, although the aggregation number does increases and hydration decreases at higher temperatures in such a way that the effective hard sphere diameter stays roughly constant. The sharp increase in SANS intensity at small k is mainly due to divergence of

the structure factor $S(k)$ as result of the critical fluctuation. Although Baxter solution of the sticky hard sphere model is mean field like, it is able to describe the critical scattering satisfactorily for temperatures further than one degree away from the critical point. The commercial L64 sample we obtained contains considerable amount of hydrophobic impurities and, therefore, the critical point is not sharply defined. However, upon purification the critical point becomes sharper and the rate of phase separation above the critical temperature much faster. New results of this paper are: (a) the critical concentration fluctuation is associated with an unusually large short-range correlation length $\xi_0 = 61$ Å; (b) we successfully map the sticky hard sphere phase diagram to the experimental phase diagram of the L64/D_2O system, and (c) the kinetic glass transition line at high concentrations identified by our dynamic light scattering experiment done previously seems to coincide with points in the phase diagram where sudden narrowing of the structural correlation peak observed by our latest SANS experiments.

Acknowledgements

We are happy to contribute this article to this special issue marking the 65th birthday of Professor Heinz Hoffmann who has also contributed so much to the studies of phase behavior and self-assembled structures in Pluronic solutions over the years. This research is supported by a grant from Materials Research Division of US DOE. We acknowledge with gratitude SANS beam time given to us by Center for Neutron Research of NIST, and Intense Pulse Neutron Source Division of ANL.

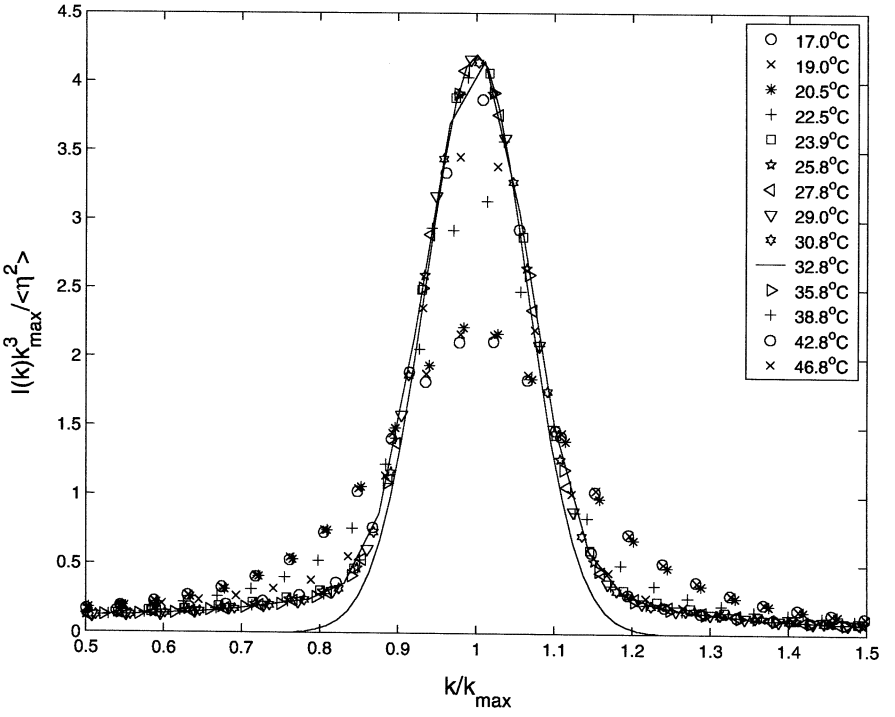

Fig. 9. A scaling plot of SANS intensity distributions at 50 wt.% concentration (purified samples) and different temperatures. It is easily seen that there is a sharp transition in line width occurring at around $T = 22.5$°C. Solid line represents the k resolution of SANS spectrometer used.

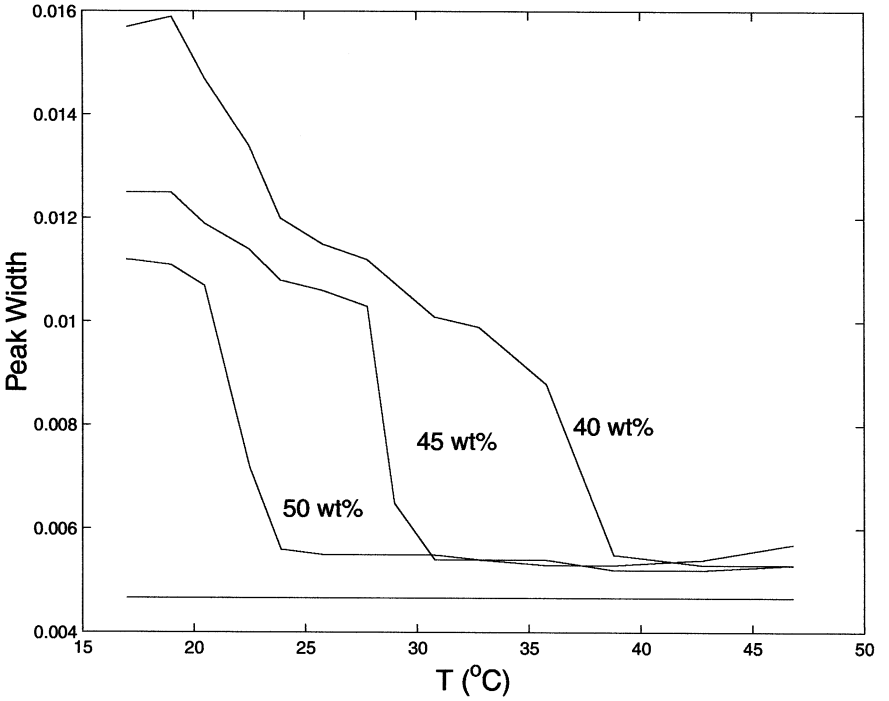

Fig. 10. The line shape of the scaled intensity distribution is approximately Lorentzian. This is a plot of the half widths of the Lorentzian line as function of temperature at different concentrations. The dotted line represents the width of the resolution function.

References

[1] B. Lindman, A. Carlsson, G. Karlstrom, M. Malmsten, Adv. Coll. Interf. Sci. 32 (1990) 183.
[2] Pluronic and Technical Brochure For Tetronic Surfactants. BASF Corp., Parsipanny, NJ (1989).
[3] P. Alexandridis, T.A. Hatton, Coll. Surf. 96 (1995) 1.
[4] B. Chu, Langmuir 11 (1995) 414.
[5] G. Wanka, H. Hoffmann, W. Ulbricht, Macromolecules 27 (1994) 4145.
[6] Z. Zhou, B. Chu, J. Coll. Interf. Sci. 126 (1988) 171.
[7] W. Brown, K. Schillen, M. Almgren, S. Hvidt, P. Bahadur, J. Phys. Chem. 95 (1850) 1991.
[8] K. Schillen, W. Brown, R.M. Johnsen, Macromolecules 27 (1994) 4825.
[9] K. Mortensen, Prog. Coll. Polymer Sci. 91 (1993) 69.
[10] M. Almgren, J. Alsins, P. Bahadur, Langmuir 7 (1991) 446.
[11] M. Almgren, W. Brown, S. Hvidt, Coll. Polymer Sci. 273 (1995) 2.
[12] K. Mortensen, W. Brown, E. Jorgensen, Macromolecules 27 (1994) 5654.
[13] Y.C. Liu, Microstructure of Micelles Formed by Tri-Block Copolymer in Water and Relation to Rheology of Solutions, PhD thesis, MIT (March, 1997).
[14] Y.C. Liu, S.H. Chen, J.S. Huang, Macromolecules 31 (1998) 2236–2244.
[15] R.J. Baxter, J. Chem. Phys. 49 (1968) 2770–2774.
[16] J.K. Percus, G.J Yevick, Phys. Rev. 110 (1958) 1–13.
[17] B. Barboy, J. Chem. Phys. 61 (1974) 3194–3197.
[18] Y.C. Chiew, E.D. Glandt, J. Phys. A Math. Gen. 16 (1983) 2599.
[19] S.H. Chen, J. Rouch, F. Sciortino, P. Tartaglia, J. Phys. Condens. Matter 6 (1994) 10855–10883.
[20] M. Kotlarchyk, S.H. Chen, J. Chem. Phys. 79 (1983) 2461.
[21] P.R. Bevington, Data Reduction and Error Analysis for the Physical Sciences, McGraw-Hill, New York, 1969.
[22] P. Linse, Macromolecules 27 (1994) 2685.
[23] A.A. Al-Saden, T.L. Whateley, A.T. Florence, J. Coll. Interf. Sci. 90 (1982) 303–309.
[24] Z. Zhou, B. Chu, Macromolecules 21 (1988) 2548–2554.
[25] K. Pandya, P. Bahadur, T.N. Nagar, A. Bahadur, Coll. Surf. A Physicochem. Eng. Aspects 70 (1993) 219–227.
[26] L. Lobry, N. Micali, F. Mallamace, C. Liao, S.H. Chen, Phys. Rev. E 60 (1999) 7076–7087.

[27] K. Mortensen, J. Phys. Condens. Matter 8 (1996) A103–A124.
[28] K. Mortensen, J.S. Pederson, Macromolecules 26 (1993) 805–812.
[29] K.N. Reddy, P.J. Fordham, D. Attwood, C. Booth, J. Chem. Soc. Faraday Trans. 86 (1990) 1569.
[30] M.J. Kositza, C. Bohne, P. Alexandridis, T.A. Hatton, J.F. Holzwarth, Langmuir 15 (1999) 322.
[31] C. Liao, S.M. Choi, F. Mallamace, S.H. Chen, J. Appl. Crystallogr. 33 (2000) 677–681.
[32] F. Mallamace, P. Gambadauro, N. Micali, P. Tartaglia, C. Liao, S.H. Chen, Phys. Rev. Lett. 84 (2000) 5431–5434.